Analysis of Critical-State Problems in Type-II Superconductivity

Leonid Prigozhin

Abstract—**An efficient numerical scheme is proposed for modeling the hysteretic magnetization of type-II superconductors. Numerical examples are presented for the Bean and Kim critical state models. It is shown that Bean's model is a Hele–Shaw type problem.**

***Index Terms*—Critical current, high-temperature superconductors, magnetization, numerical analysis, variational methods.**

I. Introduction

SOLUTION of critical-state problems for samples of arbitrary shape, especially those with high demagnetizing factors, is a matter of current interest in applied superconductivity. In this paper, we consider the solution of these problems for two-dimensional and axially symmetric configurations. For such configurations, the electric field and current density in a superconductor are parallel and the critical-state model may be characterized by a scalar current–voltage relation (the material is assumed isotropic).

The first critical-state model has been proposed by Bean (see [1]) and it is still most often employed for simulating the magnetization of type-II superconductors. In this model, the superconducting material is characterized by a nonsmooth multivalued $E(J)$ graph: the current density cannot exceed some critical value J_c and, until this threshold is reached, the electric field is zero [Fig. 1(a)].

The Bean model leads to a free boundary problem which was studied mathematically in [2]. It was, in particular, shown that the effective resistivity of superconductor in this quasi-stationary model is a Lagrange multiplier related to the current density constraint.

Generalizations and approximations of Bean's current–voltage law for a superconductor have been proposed by many authors. Kim *et al.* [3] showed that the critical current density depends on the magnetic induction. The material transition into the normal state at a point where the effective resistivity of superconductor reaches its resistivity in the normal state [Fig. 1(b)] may be introduced into the Bean model to make it more realistic. The power law [Fig. 1(c)]

$$E = E_c|J/J_c|^{m-1}J/J_c \tag{1}$$

often served either as a smooth approximation of $E(J)$ relation in the critical-state models (with $m \sim 20 - 100$) or, with a

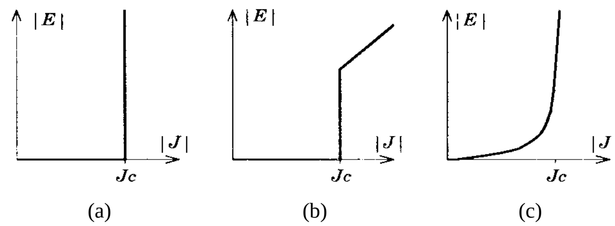

Fig. 1. (a) Bean's model, (b) its generalization, and (c) an approximation by a power law.

smaller m, as a means to account for the thermally activated creep of magnetic flux in type-II superconductors (see, e.g., [4] and [5]).

The analytical solutions to critical-state problems are available only in special cases, see [6]–[10]. To solve these free boundary problems numerically, several front-tracking methods have been developed [11]–[13]. Such methods, although exact and efficient in some cases, are not universal. Their application is difficult if the topology of the free boundary is complicated, changes in time, or is not known *a priori*.

The universality is the advantage of the free-marching numerical schemes, like the scheme derived in our work. As in [4] and [5], we use the magnetic vector potential formulation of critical-state problems. However, instead of approximating the current–voltage relation by a power law (1), we deal with the multivalued $E(J)$ characteristic directly and arrive at a generalization of variational formulation proposed in [2]. The formulation obtained can be used for numerical solution of critical-state problems with arbitrary current–voltage laws and allows the avoidance of front-tracking.

II. Vector Potential Formulation

Let a superconductor be placed into magnetic field $\boldsymbol{H}_e(\boldsymbol{x}, t)$ induced by a given external current with density $\boldsymbol{J}_e(\boldsymbol{x}, t)$. We limit our consideration to configurations that are either axially symmetric (and then denote by Ω half the cross section of superconductor), or two-dimensional (cylindrical superconductor with the cross section Ω in a perpendicular field). As a simplification, we neglect the Meissner current and assume that the lower critical field H_{c_1} is zero and $\boldsymbol{B} = \mu_0\boldsymbol{H}$, where $\boldsymbol{B}$ is the magnetic induction, $\boldsymbol{H}$ is the magnetic field, and μ_0 is the permeability of vacuum.

In the case of cylindrical superconductor in a perpendicular external field, the vectors of current density in the superconductor and of external current density $\boldsymbol{J}$ and $\boldsymbol{J}_e$ are directed along the cylinder (parallel to z axis). The same is true for

Manuscript received May 28, 1997. This work was supported by the Feinberg Fellowship.

The author is with the Department of Applied Mathematics and Computer Sciences, Weizmann Institute of Science, Rehovot 76100, Israel.

Publisher Item Identifier S 1051-8223(97)08897-0.

1051–8223/97$10.00 © 1997 IEEE

the magnetic vector potential $\boldsymbol{A} = \boldsymbol{A}_i + \boldsymbol{A}_e$ if the potentials of induced and external currents $\boldsymbol{A}_i$ and $\boldsymbol{A}_e$ are chosen as convolutions of the current densities $\boldsymbol{J}$ and $\boldsymbol{J}_e$ with the Green's function of Laplace equation $\mathcal{G} = -(1/2\pi)\,\log(|\boldsymbol{x} - \boldsymbol{x}'|)$

$$\begin{aligned} \boldsymbol{A}_i &= \mu_0 \int \mathcal{G}(\boldsymbol{x}, \boldsymbol{x}')\boldsymbol{J}(\boldsymbol{x}', t)\, d\boldsymbol{x}' \\ \boldsymbol{A}_e &= \mu_0 \int \mathcal{G}(\boldsymbol{x}, \boldsymbol{x}')\boldsymbol{J}_e(\boldsymbol{x}', t)\, d\boldsymbol{x}'. \end{aligned} \tag{2}$$

This choice corresponds to the Coulomb gauge $\nabla \cdot \boldsymbol{A} = 0$ and $\boldsymbol{A}$ satisfies the equation

$$-\Delta \boldsymbol{A} = \mu_0(\boldsymbol{J} + \boldsymbol{J}_e). \tag{3}$$

Inside the superconductor, the electric field $\boldsymbol{E}$ is induced by the movement of magnetic vortices and is parallel to the current density. This field can be expressed via the vector and scalar potentials [14]

$$\boldsymbol{E} = -\partial_t \boldsymbol{A} - \nabla V. \tag{4}$$

Since both $\boldsymbol{E}$ and $\boldsymbol{A}$ are directed along the z axis and do not depend on z, this equation can be satisfied only if $\nabla V = C(t)\boldsymbol{e}_z$ and so (4) becomes scalar. Specifying the current–voltage law for the superconductor and taking (2) into account, we obtain

$$E + \partial_t(A_i[J] + A_e) = -C(t), \qquad E \in E(J). \tag{5}$$

Although the cylinder is supposed to be long, its length is finite. Therefore, if no transport current is fed into the superconductor, the current in the positive direction of the z axis must return as a negative current. The additional condition

$$\int_\Omega J = 0$$

fixes the time-dependent constant $C(t)$.

Problems in which the applied transport current $I_{\rm tr}(t)$ is not zero are also of much practical interest for this configuration. In such cases, $C(t)$ is determined by the condition

$$\int_\Omega J = I_{\rm tr}(t). \tag{6}$$

In axisymmetric case, we use the cylindrical coordinates (r, z, ϕ) and $\boldsymbol{x} = (r, z)$ as coordinates of cross section points. The function $\mathcal{G}$ in (2) can be expressed using the complete elliptic integrals of the first and second kind, $K(k)$ and $E(k)$

$$\mathcal{G} = \frac{1}{\pi k}\sqrt{\frac{r'}{r}}\left\{K(k)\left(1 - \frac{k^2}{2}\right) - E(k)\right\}$$

where

$$k^2 = \frac{4r\,r'}{(r + r')^2 + (z - z')^2}.$$

Equation (4) is scalar also in this case, since only the ϕth coordinates of $\boldsymbol{J}$, $\boldsymbol{A}$, and $\boldsymbol{E}$ are nonzero. It is not difficult to see that now $\nabla V = \{C(t)/r\}\boldsymbol{e}_\phi$ and we must choose $C(t) = 0$, because otherwise the electric field becomes infinite at $r = 0$.

Thus we obtain the following formulation for the axisymmetric critical-state problems:

$$E + \partial_t(A_i[J] + A_e) = 0, \qquad E \in E(J). \tag{7}$$

Additionally, the initial current density must be given

$$J|_{t=0} = J_0(\boldsymbol{x}). \tag{8}$$

Several remarks about the formulations obtained seem appropriate.

Equations (5), (6), (8), and (7), (8) should be solved only inside the superconductor, where the current–voltage relation is determined by a critical-state model. The electric field in the exterior space is irrelevant and remains undetermined.

If the electric field in a superconductor were determined by the local values of current density in a unique way, as is true for the current–voltage law on Fig. 1(c), we could write $E = E(J)$ in (5) and (7). Brandt [4], [5] used the power law approximation (1) with $m \gg 1$ to simulate numerically the Bean-like magnetization of a rectangular bar in a perpendicular applied field. The convergence of such power-law approximations to the Bean model, as the power m tends to infinity, is an interesting question which we discuss at the end of this paper.

Generally, the model $E(J)$ dependence may be multivalued [see Fig. 1(a) and (b)]. Provided this law is a monotone graph, the solution of critical-state problem may be sought as a pair of functions $\{E, J\}$ satisfying (5), (6), (8) or (7), (8).

For zero transport current, (6) is almost automatically satisfied with $C(t) = 0$ in (5) if the cylinder cross section is symmetric and the external field uniform. (Assuming the external field is induced by two parallel sheets of currents, one has only to place the superconductor symmetrically between the two sheets, then the condition $\int J = 0$ is a consequence of the problem's symmetry.) Only such problems have been considered in [4], [5], and [15], where (6) has not been formulated explicitly.

Applying the Laplace operator to (5), using (3), and taking into account that J_e is zero inside the superconductor, we obtain

$$\mu_0 \partial_t J - \Delta E = 0, \qquad E \in E(J). \tag{9}$$

This nonlinear differential equation looks simpler than the integro-differential relation (5). However, unlike this relation, the differential equation contains no information about the external field and transport current and has to be coupled with a nonlocal boundary condition (see below) or solved jointly with an exterior problem defined in an infinite domain. The latter method was proposed in [16] and recently realized in [17] for the same geometry as in [4] but with the constitutive laws as on Fig. 1(a) and (b). To make the calculations feasible, these multivalued $E(J)$ graphs were approximated by functions having neither infinite nor zero slopes.

An interesting numerical procedure proposed in [18] is based on a dual approach, in which the inverse relation, $J \in J(E)$, is used. Since it is difficult to distinguish between small and strictly zero electric field values if they are found numerically, an approximation of this multivalued graph is necessary in this case as well (see also [19]).

The free-marching numerical schemes based on the vector-potential formulation and mentioned above allow the solving of the critical-state problems. However, the rate of their convergence and the accuracy of solutions obtained can be sensitive to the parameters of approximation of a multivalued current–voltage law in the model of superconductor.

We will now present a numerical method that deals with these multivalued relations directly, without any approximation. Let us start with the Bean and Kim models.

III. The Bean and Kim Models

According to the Bean model, the current density J in a superconductor satisfies the condition $|J| \le J_c$ and the electric field E is zero wherever $|J| < J_c$. For $J = \pm J_c$, this model gives $E \in \pm[0, \infty)$ [see Fig. 1(a)]. Therefore, (5) simply means

$$\partial_t A_i[J] + \partial_t A_e + C(t) \begin{cases} \ge 0 & \text{if } J = -J_c \\ = 0 & \text{if } |J| < J_c \\ \le 0 & \text{if } J = J_c \end{cases}$$

where $C(t)$ is implicitly determined by (6). Let us define, for each time moment, the set of admissible current densities

$$K = \left\{ \varphi(\boldsymbol{x})\colon |\varphi| \le J_c,\ \int_\Omega \varphi = I_{\mathrm{tr}} \right\}. \tag{10}$$

We suppose $|I_{\mathrm{tr}}| \le J_c|\Omega|$, and so the set K is not empty ($|\Omega|$ means the area of Ω). Obviously, for any φ from the set K

$$\{\partial_t A_i[J] + \partial_t A_e + C(t)\}(\varphi - J) \ge 0$$

everywhere in Ω. Integrating this inequality and taking into account that $\int \varphi = \int J = I_{\mathrm{tr}}$, we can reformulate the critical-state problem (5), (6), (8) with the Bean $E(J)$ law as a variational inequality

$$\begin{cases} \text{Find } J \in K \text{ such that} \\ (\partial_t A_i[J] + \partial_t A_e,\ \varphi - J) \ge 0 \text{ for all } \varphi \in K, \\ J|_{t=0} = J_0. \end{cases} \tag{11}$$

Here (f, g) is the scalar product of two functions defined as $\int_\Omega fg$.

For axisymmetric problems, the variational inequality may be written in the same form but with the set of admissible functions

$$K = \{\varphi\colon |\varphi| \le J_c\} \tag{12}$$

and the scalar product of two functions defined as $\int_\Omega rfg$.

It may be noted that, although the variational formulations where the solution is sought as an extremal point of some functional are much more familiar, the variational inequalities do appear in many problems of mechanics and physics containing a unilateral constraint or a nonsmooth constitutive relation (see [20]).

A similar formulation is readily obtained for the Kim model, in which the critical current density depends on the magnetic field: $J_c = J_c(|\boldsymbol{H}|)$. Provided the current density J is known, one can find the magnetic field via the Biot–Savart law. Hence, $\boldsymbol{H} = \boldsymbol{H}[J]$ and the set of admissible functions in the variational inequality, K, itself depends on the unknown solution. This is an additional nonlinearity: we need to find J such that it belongs to $K[J]$ and the inequality in (11) holds for all functions φ from $K[J]$. Such problems are called quasi-variational inequalities.

The numerical methods for variational inequalities are well developed [21]. We refer to [15] for the details of our numerical procedure and the comparison of numerical and analytical solutions. Here we describe briefly this numerical scheme and present some more interesting examples.

If $K = K[J]$, the finite-difference approximation of (11) in time leads, for each time layer, to the stationary quasi-variational inequality

$$\begin{gathered} \text{Find } J \in K[J] \text{ such that} \\ (A_i[J] - A_i[\hat{J}] + A_e - \hat{A}_e,\ \varphi - J) \ge 0 \\ \text{for all } \varphi \in K[J] \end{gathered} \tag{13}$$

where $\hat{J}$ and $\hat{A}_e$ are the values taken from the previous time layer. It can be shown that the inequalities (13) are equivalent to optimization problems with an implicit constraint

$$\mathcal{F}[J] = \min_{\varphi \in K[J]} \mathcal{F}[\varphi] \tag{14}$$

where

$$\mathcal{F}[J] = \tfrac{1}{2}(A_i[J],\ J) - (A_i[\hat{J}] - A_e + \hat{A}_e,\ J)$$

is a quadratic functional.

To solve (14), we apply an iterative scheme,

$$\mathcal{F}[J^{(n+1)}] = \min_{\varphi \in K[J^{(n)}]} \mathcal{F}[\varphi] \tag{15}$$

and discretize (15) in space using the method of finite elements (piecewise constant elements are most convenient here). Finally, we solve numerically the resulting problems of convex programming.

To calculate the constraint in (15), it is necessary to find first the magnetic field corresponding to current density from the previous iteration, $J^{(n)}$. This can be done (for each finite element) by simply summing up the fields induced by the currents of other elements and adding the field of external current. These iterations are not needed for the Bean model, since the critical current density in this model is fixed.

For axisymmetric problems, where only the point-wise current density constraint should be taken into account [see (12)], the optimization problem (15) can be efficiently solved using a modification of the point relaxation method [15]. In the cylindrical case, where an additional integral constraint arises [see (10)], this algorithm can be combined with the Lagrange multiplier method to resolve all constraints iteratively. At the ith iteration, given the Lagrange multiplier $C = C^i$, the point relaxation method is used to determine J^i, the minimal point of

$$F[J] + C\left(\int_\Omega J - I_{\mathrm{tr}}\right)$$

on the set of functions satisfying the current density constraint $|J| \le J_c$. Then a new approximation to the Lagrange multiplier C is calculated in accordance with

$$C^{i+1} = C^i - \kappa\left(\int_\Omega J^i - I_{\mathrm{tr}}\right) \tag{16}$$

where κ is a constant. These iterations are performed until the integral condition is satisfied with the given tolerance.

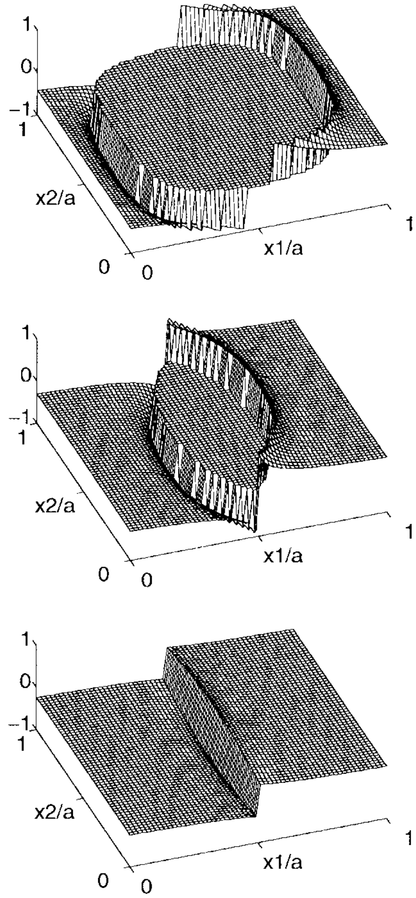

Fig. 2. Normalized current density J/J_{c0} computed using Kim's model $[J_c = J_{c0}H_K/(H + H_K),\ H_K = 0.05aJ_{c0}]$ for cylindrical superconductor with square $a \times a$ cross section in a growing perpendicular field $H_e/aJ_{c0} = 0.05, 0.10, 0.15$.

IV. Numerical Examples

We assume that the superconductors initially are in a virgin state, $J_0 = 0$, and consider first the magnetization of a cylindrical superconductor with square cross section in a uniform perpendicular external field $\boldsymbol{H}_e = H_{e,1}(t)\boldsymbol{i}_1 + H_{e,2}(t)\boldsymbol{i}_2$. This field in the neighborhood of superconductor can be generated by two parallel sheets of current and the corresponding magnetic potential is $A_e = x_2H_{e,1} - x_1H_{e,2}$. No transport current is applied.

The first example demonstrates a solution of quasi-variational inequality corresponding to Kim's model (Fig. 2).

As the external field, parallel to the x_2 axis, grows, the shielding regions of plus and minus critical current appear at the boundary and propagate inside the superconductor. The zero field core shrinks and eventually disappears. At each time layer, the convergence in (15) has been achieved after four to five iterations.

Qualitatively, the solution obtained is similar to the Bean model solution [5], [15], and we will use the Bean model in other examples below. Note, however, that the critical current density in Kim's model decreases with the growth of magnetic field and this explains the shape of computed hysteresis loops of magnetic moment $\boldsymbol{M} = \int_\Omega \boldsymbol{x} \times \boldsymbol{J}$ (Fig. 3).

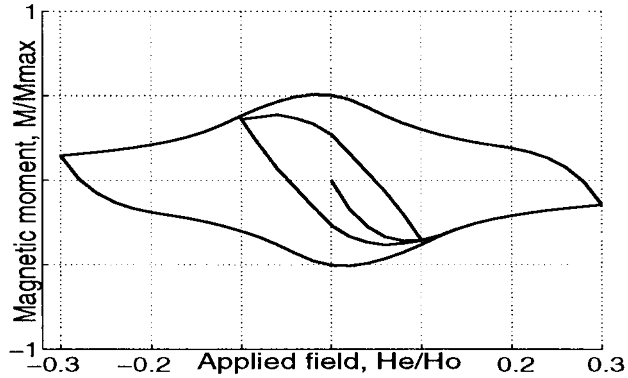

Fig. 3. The hysteresis loops for Kim's model. Magnetic moment $M/M_{\max}$ versus applied magnetic field H_e/H_0; $H_0 = aJ_{c0}$, $M_{\max} = a^2J_{c0}/4$.

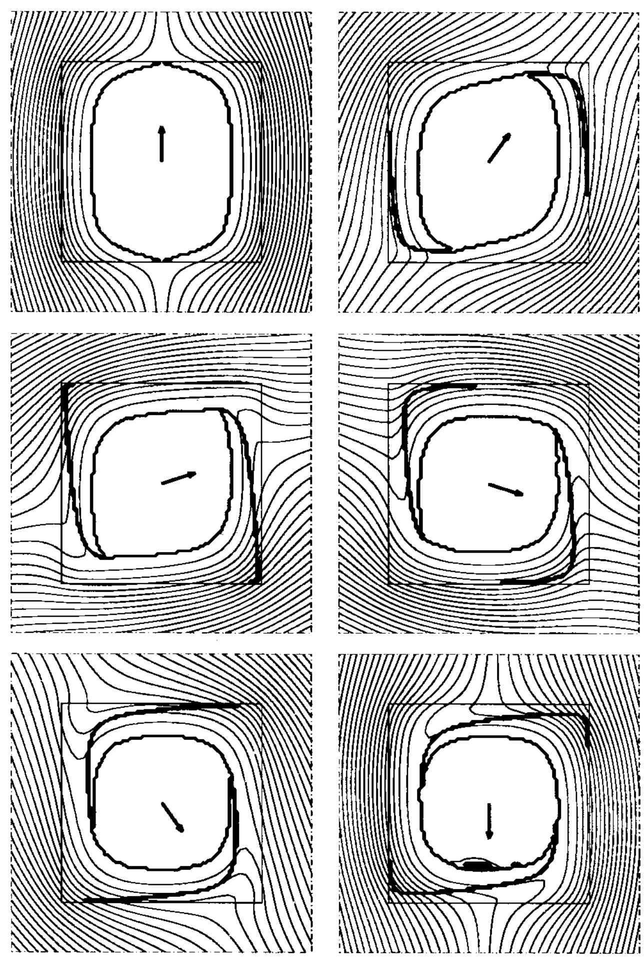

Fig. 4. Penetration fronts and magnetic field lines, Bean's model. Long superconductor with square $a \times a$ cross section in a perpendicular field which first grows up to $H_e/aJ_c = 0.1$, then rotates. Arrows show the direction of external field.

The evolution of magnetized state in a rotating perpendicular field was calculated for the same sample (Fig. 4). In this case we assumed the Bean model and solved the variational inequality. The lines of magnetic field in this picture are drawn as the level contours of magnetic potential A.

As it was explained above, the zero transport current condition in these two examples is satisfied with $C(t) = 0$

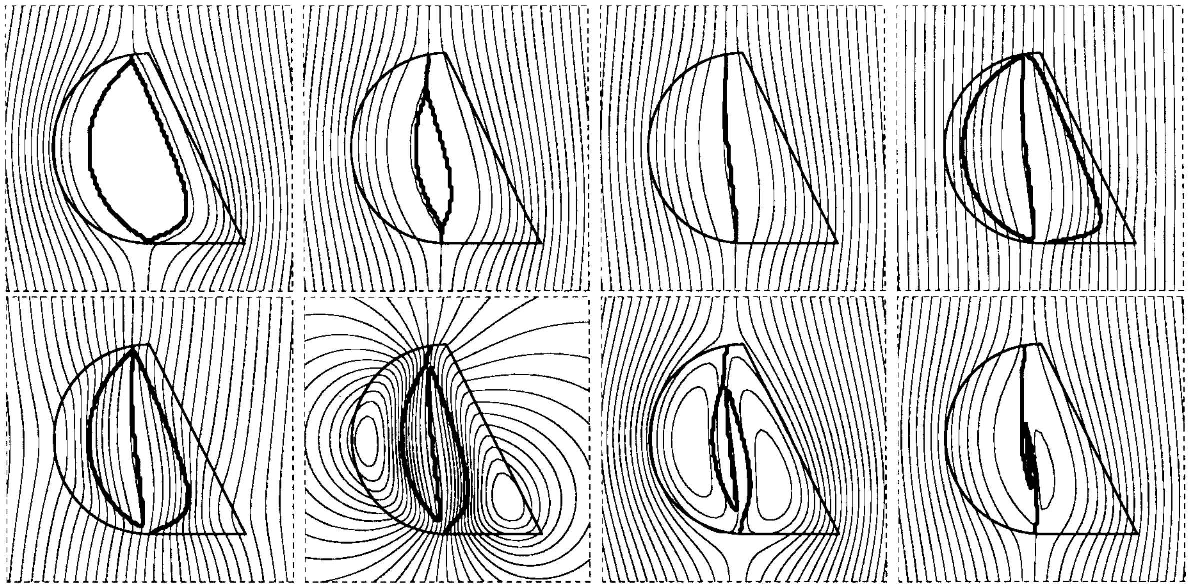

Fig. 5. Cylindrical superconductor with an asymmetric cross section; penetration fronts and magnetic field lines. The uniform external magnetic field is directed vertically, $H_e/aJ_c = 0.1, 0.2, 0.3, 0.2, 0.1, 0.0, -0.1, -0.2$ (a is the cross section height).

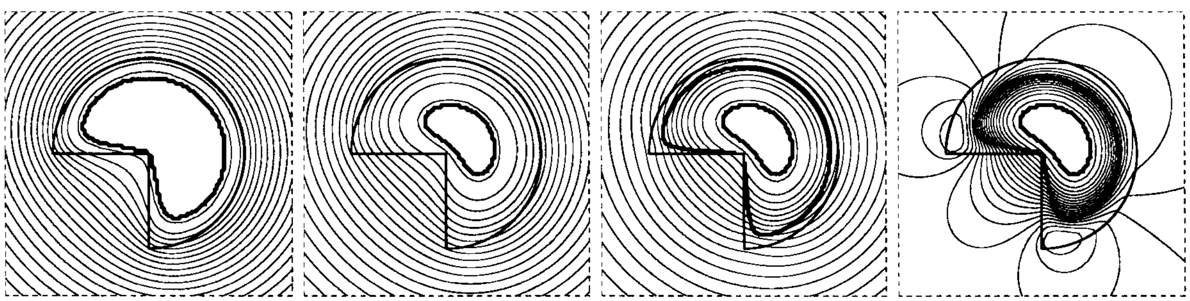

Fig. 6. Penetration fronts and magnetic field lines. Cross section is a sector with the radius R and central angle $3\pi/2$. The transport current: $I_{\rm tr}/JcR^2 = 1, 2, 1, 0$.

in (5) due to the symmetry of the cross section and the chosen external potential. In such cases the integral constraint in (10) may be omitted. In the general case, however, this condition is necessary and we took it into account to simulate the magnetization of a cylindrical superconductor with an asymmetric cross section (Fig. 5). Also, in this example no transport current is applied. The external uniform magnetic field first grows, and the zero field core shrinks as the regions of shielding critical currents propagate inside the superconductor. Then, as the external field decreases, the current density changes its direction near the sample surface. The moving boundary between regions of plus and minus critical current densities becomes really complicated in this case.

Let us now consider a problem with the transport current and zero external field (Fig. 6). Numerical simulation shows that, as the transport current increases, an expanding region of the critical current density appears near the sample surface; this region surrounds a shrinking zero field (and zero current) core. The boundary of the core remains stationary as the applied current decreases, but a new front appears at the sample surface and a region of the opposite critical current starts to propagate inside the superconductor. In this and the previous example, the Lagrange multiplier technique (16) was used with $\kappa = 0.3$. Not more than five to eight iterations were needed.

The next two examples (Figs. 7 and 8) show axisymmetric magnetization of two samples, a hollow ball and a cone, in a growing external field. This uniform field $\boldsymbol{H}_e = H_e(t)\boldsymbol{i}_z$ generated inside a long solenoid corresponds to magnetic potential $A_e = rH_e/2$. In this geometry, the magnetic field lines can be drawn as the contours of rA.

As the last example, let us consider the magnetization of an infinite tape. A solution to this problem has been recently presented in [22] and we will use the same set of parameters. Let a coil of radius $R_c = 1.0$ mm be parallel to the surface of an infinite superconducting tape of thickness 0.2 mm and placed at a height 0.4 mm above the tape surface. The magnetic field induced by the coil current I penetrates the tape and may be felt in the half-space below the tape if this current is strong enough (Fig. 9). In this case, the external field is not uniform and a known expression for the potential of coil current should now be substituted into the variational inequality.[1]

As the penetration front reaches the tape lower surface, the front breaks into two parts. To account for this change

[1] A_e can be found as $\int \mathcal{G} J_e$ with the delta-function external current.

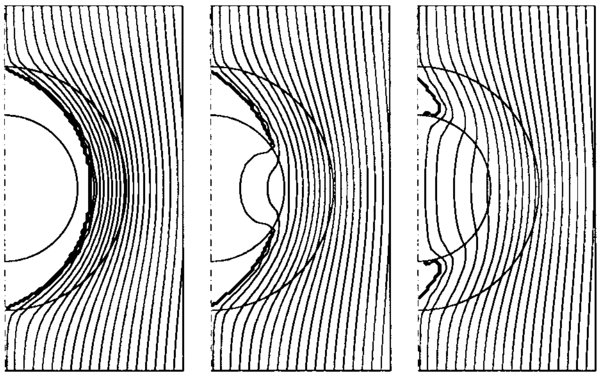

Fig. 7. Magnetization of a hollow ball, Bean's model. External field $H_e/RJ_c = 0.2, 0.3, 0.4$.

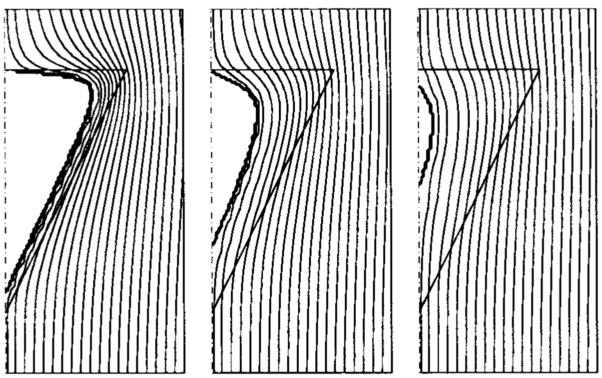

Fig. 8. Magnetization of a cone, Bean's model. External field $H_e/RJ_c = 0.1, 0.3, 0.5$.

of free boundary topology, Koo and Telschow [22] derived two different front-tracking algorithms, similar to that in [13]. For each value of coil current, the fronts were sought as the functions of radial coordinate $z = \Psi(r)$. However, such a representation is not possible after the breaking point (see Fig. 10), and so only the first part of the solution [22] is correct.

This example demonstrates the advantage of free-marching numerical schemes: they do not need any *a priori* information about the free boundary behavior and are applicable without modifications even if the topology of free boundary changes with time.

Another important feature of the presented numerical method is that all the calculations are confined to the region of superconductor. Solving an exterior problem (see [16] and [17]) seems to us more difficult and less efficient than solving the variational inequality (11) with a nonlocal operator.

V. General Current–Voltage Relations

The numerical scheme presented above for the Bean and Kim models may be generalized for models with arbitrary current–voltage laws. For simplicity, we consider the constitutive laws which do not depend on the magnetic field.

Let us assume $E(J)$ is a monotone graph and, following Bossavit [16], define a function $u(J) = \int_0^J E(s)\,ds$ and a convex functional $\mathcal{U}[J] = \int_\Omega u(J)$ for two-dimensional, $\mathcal{U}[J] = \int_\Omega u(J)r$ for axisymmetric configurations. It can be

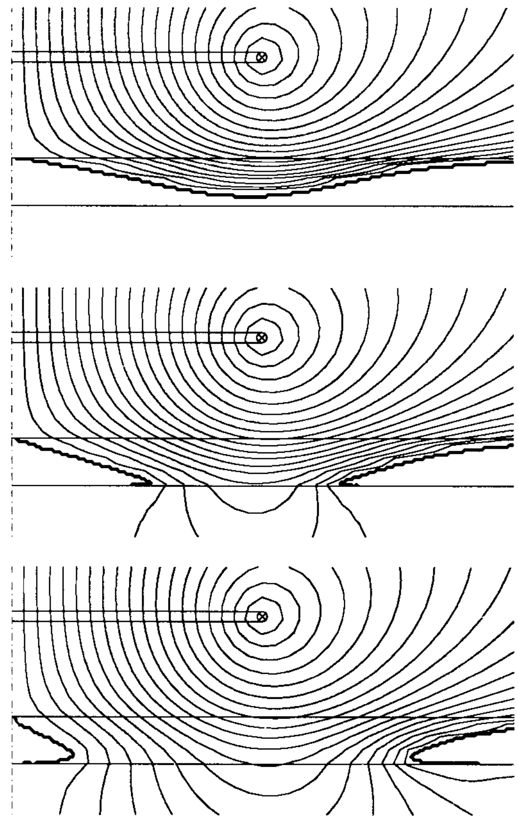

Fig. 9. Magnetization of superconducting tape, Bean's model. Left edge of pictures is the central axis of the coil. Coil current: $I/J_cR_c^2 = 0.3, 0.5, 0.7$.

shown that $E \in E(J)$ everywhere in Ω if and only if

$$\mathcal{U}[J'] - \mathcal{U}[J] \geq (E,\, J' - J)$$

for any J' (the electric field E is a subgradient of the functional $\mathcal{U}$, see [16]).

For axisymmetric problems, using (7) we immediately obtain that J satisfies the variational inequality

$$\mathcal{U}[J'] - \mathcal{U}[J] + (\partial_t A_i[J] + \partial_t A_e,\, J' - J) \geq 0 \qquad (17)$$

for any test function J'. To solve this variational inequality numerically, it is convenient to start with the implicit finite difference approximation of (17) in time and to seek, at each time layer, such current density J that

$$\tau(\mathcal{U}[J'] - \mathcal{U}[J]) + (A_i[J] - A_i[\hat{J}] + A_e - \hat{A}_e\,,\, J' - J) \geq 0$$

for any J' (here τ is the time step). Using standard convex analysis arguments, it is easy to show that the problem obtained is equivalent to the optimization problem

$$\min_J \{\tau \mathcal{U}[J] + \mathcal{F}[J]\} \qquad (18)$$

where $\mathcal{F}$ is as in (14). After the piecewise constant finite element approximation in space, this problem can be solved numerically.

A variational inequality, similar to inequality (17), can be derived for the current density in cylindrical superconductors if we additionally demand that the solution and test functions satisfy the constraint (6). Indeed, then $(C(t),\, J' - J) = 0$ and

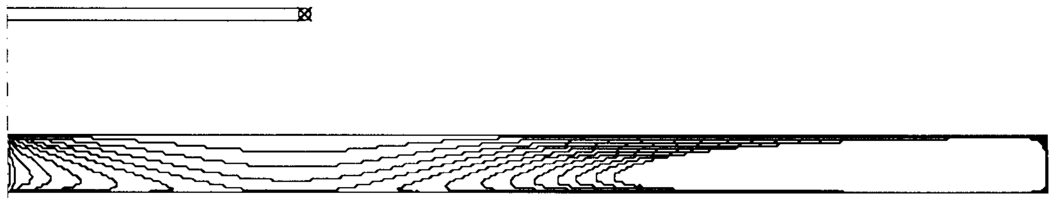

Fig. 10. Penetration fronts. $I/J_cR_c^2 = 0.1, 0.2, \cdots, 1.3$.

the inequality can be derived as this was done above. Correspondingly, for the cylindrical configuration, optimization in (18) should be performed over the set of functions satisfying (6).

Note that the time step appears in the optimization problem (18), although in (14) it does not. This is because the critical-state problems are rate independent only in case of a Bean-like $E(J)$ constitutive law [Fig. 1(a)]. For this law

$$\mathcal{U}[J] = \begin{cases} 0, & \text{if } |J| \le J_c \text{ in } \Omega, \\ \infty, & \text{otherwise} \end{cases}$$

and (14) is recovered. For $E(J)$ laws as on Fig. 1(b) and (c), the functional $\mathcal{U}$ is finite for any current.

VI. Bean's Model as a Hele–Shaw Problem

Although the variational reformulation of Bean's model is convenient for numerical solution, a different representation offered below leads, possibly, to a deeper insight into this model.

Let us consider first the magnetization model with a power current–voltage law (1). With this law, (9) is the porous medium equation. Instead of coupling (9) with an exterior problem, we may employ (5) as a nonlocal boundary condition

$$\{E + \partial_t A_i[J] + \partial_t A_e + C(t)\}|_{\partial\Omega} = 0 \qquad (19)$$

where $E = E(J)$, $\partial\Omega$ is the boundary of Ω, and the unknown C is determined by (6). Equivalently, since

$$\begin{aligned}\partial_t A_i[J] &= \mu_0 \int_\Omega \mathcal{G}\partial_t J = \int_\Omega \mathcal{G}\Delta E \\ &= \int_{\partial\Omega} [\mathcal{G}\partial_n E - E\partial_n \mathcal{G}] - E\end{aligned}$$

we can write this condition as

$$\left\{\partial_t A_e + C(t) + \int_{\partial\Omega} [\mathcal{G}\partial_n E - E\partial_n\mathcal{G}]\right\}\bigg|_{\partial\Omega} = 0. \qquad (20)$$

Let us assume

$$|J_0| \le J_c \qquad (21)$$

and consider the behavior of this problem solution as the power m in (1) tends to infinity. Such limit of the porous medium equation is well studied for the Cauchy problem, and our asymptotic arguments below may be compared with those in [23]. However, in our case the dynamics are governed by a nonhomogeneous boundary condition and the limiting solution is not stationary (for the Cauchy problem such solution is trivial, $J \equiv J_0(\boldsymbol{x})$, if (21) is satisfied).

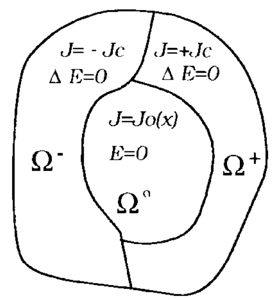

Fig. 11.

Using the normalized variables $j = J/J_c$ and $e = E/E_c$ and inverting the current–voltage relation (1), we can rewrite (9) as $\tilde{\mu}_0\partial_t j(e) = \Delta e$, where $j(e) = |e|^{1/m}\,\mathrm{sign}(e)$ and $\tilde{\mu}_0 = \mu_0 J_c/E_c$. Differentiating, we obtain

$$\frac{\tilde{\mu}_0}{m}\,|e|^{1/m}\partial_t e = |e|\Delta e$$

and, putting formally $m = \infty$, arrive at the equation $e\Delta e = 0$, or $E\Delta E = 0$. Also, the limit of $j(e)$ power law yields the Bean model relation between E and J, therefore $|J| \le J_c$ and $J = J_c\,\mathrm{sign}(E)$ if $E \ne 0$. Note also that if $|J| < J_c$ the diffusion of current in (9) is extremely slow for large m, so $\partial_t J \approx 0$, and the current density does not change.

These arguments suggest that, as $m \to \infty$, the domain Ω breaks into subdomains, Ω^+, Ω^-, and Ω^0 in which the current density tends to $+J_c$, $-J_c$, and $J_0(\boldsymbol{x})$, respectively (Fig. 11). In each subdomain, the limiting electric field satisfies the equation

$$\Delta E = 0 \qquad (22)$$

and the continuity of this field is ensured by the condition

$$E = 0 \qquad (23)$$

on the moving boundaries between the subdomains. Since (9) is a conservation law, at these free boundaries the following balance relation also holds:

$$[\partial_n E] = -\mu_0 [J] v_n. \qquad (24)$$

Here [.] is the jump across the boundary, and v_n is the normal velocity of the boundary. Equations (22)–(24) supplemented by the nonlocal boundary condition (20) form a Hele–Shaw type problem.

Additionally, the following rule has to be postulated: a new free boundary appears at $\partial\Omega$, and a new subdomain starts to grow, whenever the boundary value of E would otherwise contradict Bean's $E(J)$ law. Note that in each subdomain E

takes its minimal and maximal values at the boundary. Since $E = 0$ on the free boundaries, the formulated rule ensures $E \in E(J)$ everywhere.

No attempt to prove the convergence is made here. Instead, we will show that the vector potential formulation (5) of Bean's model can be derived from the Hele–Shaw equations.

Let $\psi(\boldsymbol{x})$ be a continuous function and φ be a solution to the Dirichlet problem

$$\Delta\varphi = \psi, \quad \varphi|_{\partial\Omega} = 0.$$

Let us multiply (22) by φ and integrate it over each subdomain Ω^i. Using the integration by parts and taking (23) and (24) into account, we obtain

$$\begin{aligned} 0 &= \sum_i \int_{\Omega^i} \varphi\Delta E \\ &= \int_\Omega E\psi - \int_{\partial\Omega} E\partial_n\varphi - \mu_0 \sum_k \int_{\Gamma^k} \varphi[J]v_n \end{aligned} \tag{25}$$

where Γ^k are the free boundaries. Since

$$\sum_k \int_{\Gamma^k} \varphi[J]v_n = \frac{d}{dt}\int_\Omega \varphi J$$

and $\mu_0 J = -\Delta A_i$, the equality (25) can be easily transformed into

$$\int_\Omega (E + \partial_t A_i[J])\psi - \int_{\partial\Omega} (E + \partial_t A_i[J])\partial_n\varphi = 0.$$

Finally, using (19) and remembering that $\Delta A_e = 0$ in Ω, we arrive at

$$\int_\Omega [E + \partial_t A_i[J] + \partial_t A_e + C(t)]\psi = 0.$$

Since ψ is arbitrary, this is equivalent to (5), and hence the Bean model is a Hele–Shaw problem.

ACKNOWLEDGMENT

The author is grateful to J. W. Barrett for his critical remarks on the first version of this work and appreciates discussions with A. Bossavit, E. H. Brandt, and Y. Shtemler.

REFERENCES

[1] C. P. Bean, "Magnetization of high-field superconductors," *Rev. Mod. Phys.*, vol. 36, no. 1, pp. 31–39, 1964.
[2] L. Prigozhin, "On the Bean critical-state model in superconductivity," *Euro. J. Appl. Math.*, vol. 7, pt. 3, pp. 237–248, 1996.
[3] Y. B. Kim, C. F. Hempstead, and A. R. Strnad, "Critical persistent currents in hard superconductors," *Phys. Rev. Lett.*, vol. 9, no. 7, pp. 306–309, 1962.
[4] E. H. Brandt, "Universality of flux creep in superconductors with arbitrary shape and current–voltage law," *Phys. Rev. Lett.*, vol. 76, no. 21, pp. 4030–4033, 1996.
[5] ——, "Superconductors of finite thickness in a perpendicular magnetic field: Strips and slabs," *Phys. Rev. B*, vol. 54, no. 6, pp. 4246–4264, 1996.
[6] A. M. Campbell and J. E. Evetts, "Flux vortices and transport currents in type-II superconductors," *Adv. Phys.*, vol. 21, pp. 199–428, 1972.
[7] C. P. Bean, "Rotational hysteresis loss in high-field superconductors," *J. Appl. Phys.*, vol. 41, no. 6, pp. 2482–2483, 1970.
[8] E. H. Brandt, M. V. Indenbom, and A. Forkl, "Type-II superconducting strip in perpendicular magnetic field," *Europhys. Lett.*, vol. 22, no. 9, pp. 735–740, 1993.
[9] E. Zeldov, J. R. Clem, M. McElfresh, and M. Darwin, "Magnetization and transport currents in thin superconducting films," *Phys. Rev. B*, vol. 49, no. 14, pp. 9802–9822, 1994.
[10] P. N. Mikheenko and Y. E. Kuzovlev, "Inductance measurements of HTSC films high critical currents," *Physica C*, vol. 204, pp. 229–236, 1993.
[11] M. Ashkin, "Flux distribution and hysteresis loss in a round superconducting wire for the complete range of flux penetration," *J. Appl. Phys.*, vol. 50, no. 11, pp. 7060–7066, 1979.
[12] R. Navarro and L. J. Campbell, "Magnetic-flux profiles of high-T_c superconducting granules: Three-dimensional critical-state-model approximation," *Phys. Rev. B*, vol. 44, no. 18, pp. 10146–10157, 1991.
[13] K. L. Telschow and L. S. Koo, "Integral-equation approach for the Bean critical-state model in demagnetizing and nonuniform-field geometries," *Phys. Rev. B*, vol. 50, no. 10, pp. 6923–6928, 1994.
[14] J. D. Jackson, *Classical Electrodynamics.* New York: Wiley, 1975.
[15] L. Prigozhin, "The Bean model in superconductivity: Variational formulation and numerical solution," *J. Comp. Phys.*, vol. 129, no. 1, pp. 190–200.
[16] A. Bossavit, "Numerical modeling of superconductors in three dimensions: A model and a finite element method," *IEEE Trans. Magn.*, vol. 30, no. 5, pp. 3363–3366, 1994.
[17] M. Maslouh, F. Bouillault, A. Bossavit, and J.-C. Vérité, "From Bean's model to *H–M* characteristic of a superconductor: Some numerical experiments," *IEEE Trans. Appl. Superconduct.*, vol. 7, pp. 3797–3801, Sept. 1997.
[18] N. Takeda, M. Uesaka, and K. Miya, "Computation and experiments on the static and dynamic characteristics of high T_c superconducting levitation," *Cryogenics*, vol. 34, no. 9, pp. 745–752, 1994.
[19] H. Hashizume, T. Sigiura, K. Miya, and S. Toda, "Numerical analysis of electromagnetic phenomena in superconductors," *IEEE Trans. Magn.*, vol. 28, no. 2, pp. 1332–1335, 1992.
[20] G. Duvaut and J.-L. Lions, *Les Inéquations en Mécanique et Physique*, Paris: Dunod, 1972.
[21] R. Glowinski, J.-L. Lions, and R. Trémoliéres, *Numerical Analysis of Variational Inequalities.* North-Holland, 1981.
[22] L. S. Koo and K. L. Telschow, "Method for determining the critical-state response of superconductors in tape geometry," *Phys. Rev. B*, vol. 53, no. 13, pp. 8743–8750, 1996.
[23] C. M. Elliot, M. A. Herrero, J. R. King, and J. R. Ockendon, "The mesa problem: Diffusion patterns for $u_t = \nabla\cdot(u^m\nabla u)$ as $m \to +\infty$," *IMA J. Appl. Math.*, vol. 37, pp. 147–154, 1986.

Leonid Prigozhin received the M.Sc. degree at Moscow Institute for Electronic Industry Engineering in 1974 and the Ph.D. degree at the Ben-Gurion University of the Negev, Israel, in 1995. Both degrees are in applied mathematics.

His research interests include mathematical modeling, free boundary and variational problems, and numerical analysis. He made his postdoctoral research at the Universities of Florence and Oxford (1994 to 1995) and since then is at the Weizmann Institute of Science, Rehovot, Israel.